

Transmission electron microscopy study on Co/Fe interdiffusion in SmCo₅/Fe and Sm₂Co₇/Fe/Sm₂Co₇ thin films

Ying Zhang,^{1,2} M. J. Kramer,^{1,a)} Debjani Banerjee,³ Ichiro Takeuchi,³ and J. Ping Liu²

¹*Division of Materials Sciences and Engineering, Ames Laboratory, USDOE, Ames, Iowa 50011, USA*

²*Department of Physics, University of Texas at Arlington, Texas 76019, USA*

³*Department of Materials Science and Engineering, University of Maryland, College Park, Maryland 20742, USA*

(Received 3 June 2011; accepted 2 August 2011; published online 13 September 2011)

We demonstrate a sharp composition transition at the interface of an as-deposited SmCo₅/Fe bilayer, while annealing results in measurable Co/Fe interdiffusion near the boundary. For the annealed SmCo₅/Fe bilayer, phase separation occurs within the bcc-layer, forming regions with 3 different Fe:Co ratios. Depositing Fe between Sm-Co layers provides a realistic model for bulk systems. Co/Fe interdiffusion was observed by TEM in an annealed Sm₂Co₇/Fe/Sm₂Co₇ “sandwich” thin film, confirming Co/Fe interdiffusion as the main mechanism controlling phase chemistry in Sm-Co/Fe bulk nanocomposites. The degree of Co/Fe interdiffusion is primarily chemically driven, and the approximate 20% Fe substitution for Co is thermodynamically stable. © 2011 American Institute of Physics. [doi:10.1063/1.3634063]

I. INTRODUCTION

Nanocomposite Sm-Co/Fe materials with exchange-coupled hard phase and soft phase have the potential to achieve high energy product values.^{1–3} Fe_{1–x}Co_x alloys are ideal compounds for the soft phase, due to their very high magnetization (M_s), with Fe₆₅Co₃₅ having the highest M_s of 2.43 T compared to 2.15 T for Fe.⁴ Our recent results have shown that interdiffusion between Co and Fe in the ball-milled bulk Sm-Co/Fe nanocomposites is quite rapid, even at moderate annealing temperatures of around 500 °C.⁵ In such bulk material, even though the initial material started with pure Fe and stoichiometric Sm-Co phases, after optimal annealing, the soft phase had an average composition Fe_{60 ± 5}Co_{40 ± 5}, with about 20-nm grain size, boosting the magnetic energy product via exchange coupling in the samples.^{5,6} Studies on interfacial modification by annealing or high-temperature deposition of epitaxial Sm-Co/Fe thin film have qualitatively shown that interfacial mixing of Co with Fe can enhance magnetic properties.^{7,8} These studies demonstrate that graded composition across the boundary between the soft phase and the hard phase is a potential route to enhance exchange coupling of the two-phase nanocomposite magnets. However, no quantitative results about the Fe/Co interdiffusion of Sm-Co/Fe thin film have been reported so far. It is unclear to what extent this interdiffusion is caused by the annealing process and how it would affect BCC phase chemistry in this ternary system. A Sm-Co/Fe bilayer structure is a convenient model system for studying the exchange coupling,⁹ reducing the complexities inherent in bulk nanocomposites. In this letter, the interdiffusion between Co and Fe in the Sm-Co/Fe thin film system is investigated using analytical TEM to study diffusion in Sm-Co/Fe thin films

fabricated under different conditions. Results are then compared to bulk samples of similar composition.

II. EXPERIMENT

Sm-Co/Fe bilayers were grown by dual-gun electron-beam evaporation on MgO (110) substrates from elemental sources at a background pressure of 2×10^{-8} Torr. Two thin films with a deposition sequence MgO(110)/Cr(10 nm)/SmCo₅(90 nm)/Fe(20 nm)/Au(7 nm) were fabricated. One sample, S1, was a control, while another sample, S2, was post-annealed at 450 °C for 30 min. The Sm₂Co₇-Fe-Sm₂Co₇ configuration thin film sample was designed to mimic the diffusion structure between the hard and nanoscaled soft phases in a bulk sample, and a sequence of MgO(110)/Cr(10 nm)/Sm₂Co₇(90 nm)/Fe(20 nm)/Sm₂Co₇(90 nm)/Au(7 nm) thin film was deposited. After deposition, this sample was post-annealed at 500 °C for 30 min (labeled as S3). In all the samples, the Cr and the first Sm-Co layer were grown at 500 °C, after which the temperature was reduced at 10 °C/min to 100 °C to grow the 20 nm Fe layer. For S3, the sample temperature was increased to 500 °C again for about 15 min to grow the second Sm₂Co₇ layer.

TEM was performed on FEI Tecnai G² F20 scanning transmission electron microscopy (STEM) equipped with a post-column Gatan Imaging Filter (GIF) and high angle annular dark field (HAADF) detector. Samples for cross-section TEM investigations were prepared using a standard procedure consisting of gluing, wire saw cutting, mechanical polishing, dimpling, and ion milling. Ion milling was performed using a liquid nitrogen cooled stage to avoid the thermal influences from the ion milling process. Z-contrast images obtained in scanning mode using a high angle annular detector can distinguish the distribution of Sm-Co hard phase and Fe-Co soft phase in the thinner regions, since the image brightness is in proportion to the mean square atomic

^{a)}Author to whom correspondence should be addressed. Electronic mail: mjkrkramer@ameslab.gov.

number (Z^2). The relatively darker layer can be directly identified as the soft magnetic Fe-Co phase and confirmed by spectroscopy. These images in conjunction with simultaneous energy dispersive x ray spectroscopy (EDS) and parallel electron energy loss spectroscopy (PEELS) line scans with an electron probe size of ~ 1 nm were used to do quantitative composition analysis across these light-to-dark boundaries in HAADF images.

III. RESULTS AND DISCUSSION

The HAADF image and line scan profiles of the as-deposited SmCo_5/Fe bilayer sample (S1) are shown in Fig. 1. The Fe layer, with dark contrast between the lighter contrast Au top layer and the Sm-Co layer, can be clearly seen in the HAADF image. EDS and PEELS were performed using a step size of 1.8 nm. PEELS spectrum line scan (Fig. 1(b)), which has clear separation between the Co L_3 edge (779 eV) and Fe L_3 edge (708 eV) demonstrates the sharpness of the boundary between magnetically soft and hard phases in the as-deposited thin film. The EDS line scan profile (Fig. 1(c)) from the Fe layer to the Sm-Co layer shows that Fe suddenly decreases from ~ 100 at. % to below detectable limits at the boundary, while the Co abruptly increases to $\sim 80\%$, as expected for the SmCo_5 compound. There is negligible chemical fluctuation in the SmCo_5 layer, with the measured composition close to stoichiometric composition of SmCo_5 and no evidence of Fe interdiffusion into the Sm-Co layer. Due to scattering, the initial 1-nm probe broadens to about 4 nm near the base of the ~ 40 nm thick sample. Simulating the line scan across the boundary composition when assuming a sharp interface and 4 nm broadened beam gives the measured profile (Fig. 1(d)), confirming an atomically sharp interface in the as-deposited Sm-Co/Fe thin film.

Unlike the as-deposited S1 sample, the annealed S2 sample (Fig. 2) shows a broader transition across the magnetically hard/soft phase boundary and non-uniform compositions within these layers. Both the EDS and EELS line scans show that the magnetically soft layer has turned into chemically separated layers. Sm and Co enrichments appear near the boundary, even though the Sm:Co ratio is approximately constant at 1:5 within the interior of the hard phase layer. The initial Fe layer now consists of a top-most portion of a ~ 20 nm pure Fe layer, a ~ 5 nm Co-rich Co-Fe region, and a ~ 15 nm Fe-rich Co-Fe region. It is not surprising to see the non-equilibrium state in this sample, since the structure is far from an optimal bulk-like interface. The Fe layer has one free surface instead of being surrounded by the Sm-Co phase, limiting the diffusion pathways.¹³ So, while the data clearly shows Co interdiffusion with Fe, forming the Fe-Co intermixed layer, it is unlikely that there is a simple exchange of Fe in the bcc phase with a Co from the Sm-Co phase, as was previously observed in bulk samples and thin films annealed at lower temperature.¹⁰ First of all, the thickness of the soft layer has increased considerably by ~ 15 nm. For these chemistry and annealing conditions, the solubility of Fe into the Sm-Co phase is limited. The HAADF image and the spectroscopy both indicate non-uniform Sm-enrichment near the Cr layer (Fig. 2(a)). While a complete solid-solution exists for the Co-Fe at high temperatures, phase transitions and phase separations occur over a wide range of compositions when the temperature is decreased.¹⁴ So, while Co-Fe interdiffusion has clearly occurred under these conditions, which phases are stable appears to be dependent on the local chemistry and temperature, since these results differ from previous studies.

We next examine a sample where the Fe layer is deposited between the Sm-Co layers. Figure 3 shows the HAADF

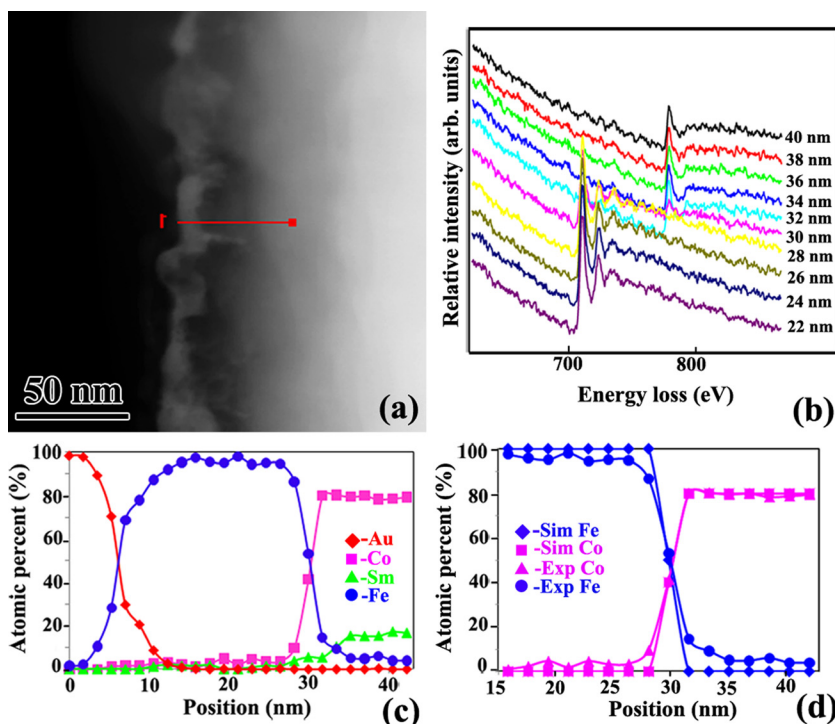


FIG. 1. (Color online) (a) HAADF image, (b) PEELS line scan, (c) EDS line scan profile, and (d) schematic illustration of the simulated and experimental composition profile across the interface between soft phase and hard phase in the as-deposited SmCo_5/Fe bilayer sample (S1).

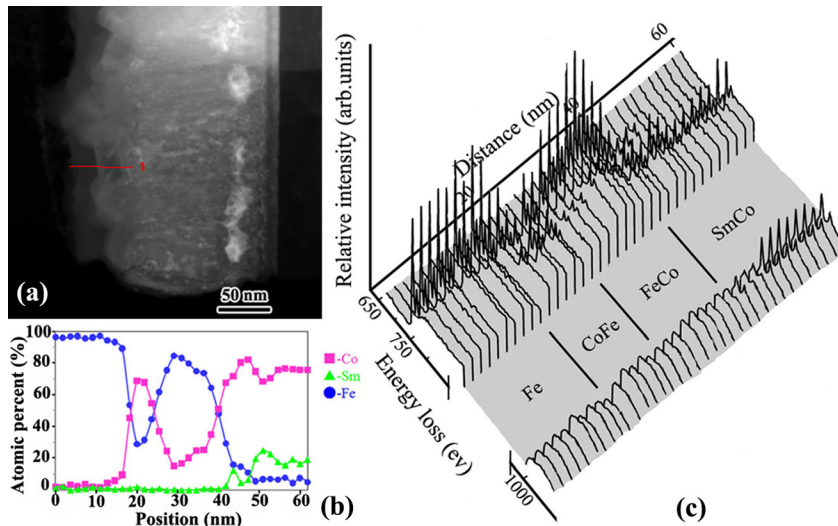


FIG. 2. (Color online) (a) HAADF image, (b) EDS, and (c) PEELS line scan profile across the soft phase layer of 450 °C annealed SmCo_5/Fe sample (S2).

image and a corresponding selected area diffraction pattern around the hard-soft phase boundary of the S3 sample. The magnetically soft phase has a darker contrast than the two SmCo layers in the HAADF image. The center portion of the film consists of textured ~ 20 nm BCC grains with the [111] zone axis sandwiched between polycrystalline Sm_2Co_7 hard phase layers. The representative EDS composition profile of the S3 sample is shown in Fig. 3(c). The EDS composition profile across the soft phase is similar to what was measured in the bulk $\text{Sm}_2\text{Co}_7/\text{Fe}$ sample.⁵ Co was found to interdiffuse across the whole 20-nm soft phase layer, and Fe was found to diffuse into the hard phase. This explains why only FeCo intermixed soft phase was observed in our previous studied bulk Sm-Co/Fe nanocomposites with the grain size about 20 nm after being annealed for 30 min at 525 °C for SmCo_5/Fe and 550 °C for $\text{Sm}_2\text{Co}_7/\text{Fe}$.⁵ The compositions are constant within the interior of the soft phase layer, indicating that local chemical equilibrium is achieved. Quantitative calculation from both EDS and PEELS profiles (PEELS is consistent with EDS, but is not shown here) shows Fe concentration increases from $\sim 20 \pm 5\%$ in the hard phase to $65 \pm 5\%$ in the BCC soft phase, while the Co concentration is approximately $35 \pm 5\%$ in the BCC phase (Fig. 3(c)). The

Co content of the soft phase is approximately the same, $40 \pm 5\%$, as was measured in the bulk nanocomposites.⁵ The slight difference is presumably due to the fact that the slightly lower annealing temperature in thin film samples induces the relatively higher Fe content in the equilibrium FeCo soft phase according to the phase diagram. The composition profiles of Co and Fe across the interface, based on both EDS and PEELS line scans, are broader than the resolution limit for the conditions used here. This supports the formation of a graded composition across the boundary. Such graded interfaces have been shown to favor exchange coupling effects in this system.^{10–12} These results further underscore that the Co-Fe interchange and a graded interface observed in bulk samples can be achieved in the Sm-Co/Fe system under the appropriate composition, phase fractions, and processing conditions. Yet, the model system is not quite perfect. We did note that there is significant composition fluctuations in the Sm_2Co_7 layer not observed in the bulk two-phase nanocomposites. Although we found slight Sm and Co enrichments near the hard-soft phase boundary in the bulk nanocomposite, the enrichments are more significant in the thin film sample. These anomalies are probably due to the need of a second 500 °C heating of the thin film required

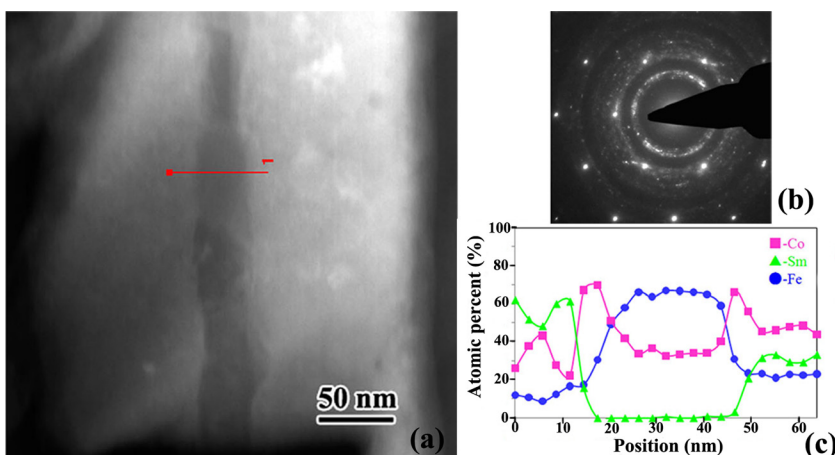


FIG. 3. (Color online) (a) HAADF image, (b) corresponding SAED pattern, and (c) EDS line scan profile across the soft phase layer of the annealed $\text{Sm}_2\text{Co}_7/\text{Fe}/\text{Sm}_2\text{Co}_7$ sample (S3).

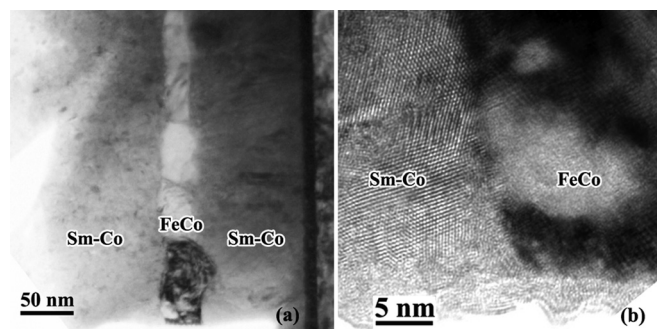


FIG. 4. (a) Bright field TEM image and (b) HRTEM image around the interface between Sm-Co hard phase and FeCo soft phase of the annealed $\text{Sm}_2\text{Co}_7/\text{Fe}/\text{Sm}_2\text{Co}_7$ sample (S3).

to deposit the top layer of the Sm_2Co_7 phase, as well as local perturbations in chemistry, which occur when switching deposition sources. The bright field TEM and HRTEM images of the S3 sample are shown in Fig. 4. The textured FeCo layer with single grains spanning the width of the layer is clearly seen between the polycrystalline Sm-Co layers (Fig. 4(a)), which is corresponding well with the selected area electron diffraction (SAED) pattern (Fig. 3(b)).

IV. CONCLUSIONS

In conclusion, in the as-deposited SmCo_5/Fe bilayer thin film, no significant Co/Fe interdiffusion was found, and the composition transition was very sharp across the interface. When the same sample was annealed at 450°C , non-equilibrium phase distributions far from the optimal bulk nanocomposite samples have been observed. However, “sandwich” structured thin film, like $\text{Sm}_2\text{Co}_7/\text{Fe}/\text{Sm}_2\text{Co}_7$, does better mimic the Co/Fe interdiffusion found in Sm-Co/Fe bulk nanocomposites.^{5,15} Compared with previous qualitative results, this study provides clear evidence that the degree of interdiffusion of Co and Fe is primarily chemically driven and the $\sim 20\%$ Fe for Co substitution in SmCo_5 and Sm_2Co_7 is thermodynamically stable. This has broad implications in design and processing nanocomposite materials,

regardless of the processing route with these materials. Rapid Co-Fe interdiffusion is responsible for the phase compositions, and the soft phase was measured to be a BCC-structured $\text{Fe}_{65\pm 5}\text{Co}_{35\pm 5}$ phase in the thin film compared with the $\text{Fe}_{60\pm 5}\text{Co}_{40\pm 5}$ phase in the annealed nanocomposites under these similar structure configuration and annealing conditions.

ACKNOWLEDGMENTS

This work was supported by the DARPA/ARO under grant W911NF-08-1-0249 and the ONR/MURI Project under Grant No. N00014-05-1-0497. Work at the Ames laboratory was supported by the U.S. Department of Energy, Office of Basic Energy Science, under Contract No. DE-AC02-07CH11358.

- ¹E. F. Kneller and R. Hawig, *IEEE Trans. Magn.* **27**, 3588 (1991).
- ²J. M. D. Coey, *Solid State Commun.* **102**, 101 (1997).
- ³R. Skomski and J. M. D. Coey, *IEEE Trans. Magn.* **30**, 607 (1994).
- ⁴I. Ohnuma, H. Enoki, O. Ikeda, R. Kainuma, H. Ohtani, B. Sundman, and K. Ishida, *Acta Mater.* **50**, 379 (2002).
- ⁵Y. Zhang, M. J. Kramer, C. B. Rong, and J. P. Liu, *Appl. Phys. Lett.* **97**, 032506 (2010).
- ⁶C. B. Rong, Y. Zhang, N. Poudyal, X. Y. Xiong, M. J. Kramer, and J. P. Liu, *Appl. Phys. Lett.* **96**, 102513 (2010).
- ⁷J. S. Jiang, J. E. Pearson, Z. Y. Liu, B. Kabius, S. Trasobares, D. J. Miller, S. D. Bader, D. R. Lee, D. Haskell, G. Srajer, and J. P. Liu, *Appl. Phys. Lett.* **85**, 5293 (2004).
- ⁸Y. Choi, J. S. Jiang, Y. Ding, R. A. Rosenberg, J. E. Pearson, S. D. Bader, A. Zambano, M. Murakami, I. Takeuchi, Z. L. Wang, and J. P. Liu, *Phys. Rev. B* **75**, 104432 (2007).
- ⁹E. E. Fullerton, J. S. Jiang, and S. D. Bader, *J. Magn. Magn. Mater.* **200**, 392 (1999).
- ¹⁰Y. Z. Liu, Y. Q. Wu, M. J. Kramer, Y. Choi, J. S. Jiang, Z. L. Wang, and J. P. Liu, *Appl. Phys. Lett.* **93**, 192502 (2008).
- ¹¹Y. Choi, J. S. Jiang, J. E. Pearson, S. D. Bader, and J. P. Liu, *Appl. Phys. Lett.* **91**, 072509 (2007).
- ¹²Z. J. Guo, J. S. Jiang, J. E. Pearson, S. D. Bader, and J. P. Liu, *Appl. Phys. Lett.* **81**, 2029 (2002).
- ¹³Y. Ustinovshikov and S. Tresheva, *Mater. Sci. Eng., A* **248**, 238 (1998).
- ¹⁴Y. Ustinovshikov, B. Pushkarev, I. Shabanova, and A. Ulianov, *Interface Sci.* **10**, 311 (2002).
- ¹⁵J. M. Le Breton, R. Larde, H. Chiron, V. Pop, D. Givord, O. Isnard, and I. Chichinas, *J. Phys. D: Appl. Phys.* **43**, 085001 (2010).